

OBSERVATIONS OF DUST AND MOLECULES IN THE DISKS AND ENVELOPES OF YOUNG STELLAR OBJECTS

MICHIEL R. HOGERHEIJDE AND EWINE F. VAN DISHOECK

Sterrewacht Leiden

P.O. Box 9513, 2300 RA Leiden, The Netherlands

AND

GEOFFREY A. BLAKE

Division of Geological and Planetary Sciences, California

Institute of Technology, MS 150-21, Pasadena, CA 91125

Abstract. Observations of dust and gas-phase molecules are compared as probes of the embedded phase of low-mass star formation. Results are presented of a detailed study of a sample of low-mass young stellar objects in Taurus with single-dish and interferometer millimeter observations. At least 67% of the objects have compact circumstellar disks, in addition to extended envelopes. HCO^+ is found to be an excellent tracer of envelope structure. Interferometer observations of its 1–0 line, and of ^{13}CO and C^{18}O , reveal the kinematics of the equatorial regions of the envelopes, and the interaction with the bipolar outflows.

1. Introduction

Emission from dust has been widely used as a tracer of star formation, as discussed in a recent overview by Chandler & Sargent (1997). An evolutionary classification has been based on the infrared spectral energy distributions of young stellar objects (YSOs), ranging from the deeply embedded class 0 and I phases, via the class II T Tauri phase, to class III pre-main-sequence stars (Lada 1987). Millimeter continuum observations have revealed the presence of circumstellar disks around $\sim 50\%$ of T Tauri stars (Beckwith *et al.* 1990; Osterloh & Beckwith 1995), together with more extended envelopes around many embedded YSOs (Keene & Masson 1990; Terebey, Chandler & André 1993; André & Montmerle 1994).

TABLE 1. Source sample

Source	IRAS PSC	Visible/ Embedded	L_{bol} L_{\odot}	M_{\star} ^a M_{\odot}	M_{disk} M_{\odot}	M_{env} M_{\odot}
L1489 IRS	04016+2610	Emb	3.70	0.4	≤ 0.004	0.016–0.025
T Tau	04190+1924	Vis+Emb	25.50	2.7	0.023	0.029
Haro 6–10	04263+2426	Vis+Emb	6.98	0.9	0.010	< 0.004
L1551 IRS 5	04287+1801	Emb	21.90	2.6	0.073	0.26
L1535 IRS	04325+2402	Emb	0.70	0.15	≤ 0.005	< 0.010
TMR 1	04361+2547	Emb	2.90	0.3	0.009	0.007
TMC 1A	04365+2535	Emb	2.20	0.3	0.020	0.018
L1527 IRS	04368+2557	Emb	1.30	0.2	0.017	0.031
TMC 1	04381+2540	Emb	0.66	0.15	≤ 0.005	0.005–0.016

^a Upper limit of stellar mass assuming objects are located on the birthline.

In addition to the spatial distribution of material and the temperature, molecular line observations also probe the density and the velocity field of the gas. This is especially interesting during the embedded phase, when the object continues to accrete matter through infall and at the same time clears its surroundings by the action of a bipolar outflow. The composition of the gas and the dust is affected by these energetic processes, evaporating icy grain mantles and destroying dust particles, thereby influencing the make-up of the primitive solar system.

2. Source sample and observations

Our study is based on a sample of nine embedded, low-mass YSOs in the Taurus–Auriga star-forming region ($d = 140$ pc), chosen by their HCO^+ $J=3-2$ emission from the IRAS flux- and colour-limited sample of Tamura *et al.* (1991). Single-dish (sub-)millimeter observations of this sample were obtained in several rotational transitions of ^{12}CO , ^{13}CO , C^{18}O , HCO^+ , and H^{13}CO^+ using the JCMT¹, the CSO², and the IRAM 30m telescope (Hogerheijde *et al.* 1997). Regions of up to $60'' \times 60''$ (10,000 AU) were mapped with beam sizes between $10''$ and $30''$ (1000–4000 AU). The observed lines trace hydrogen number densities of 10^3 – 10^7 cm^{-3} and kinetic temperatures 10–100 K. Interferometric observations of HCO^+ , ^{13}CO , and

¹The James Clerk Maxwell Telescope is operated by the Joint Astronomy Centre on behalf of the UK Particle Physics and Astronomy Research Council, the Netherlands Organization for Scientific Research and the National Research Council of Canada.

²The Caltech Submillimeter Observatory is operated by the California Institute of Technology under funding from the U.S. National Science Foundation (#AST93–13929).

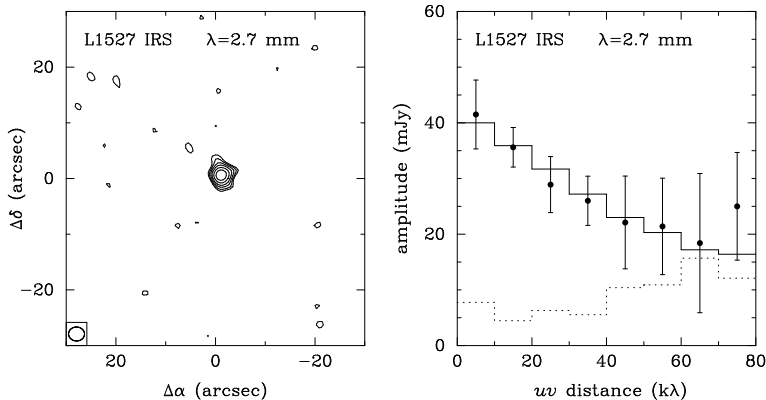


Figure 1. Left: cleaned image of 2.7 mm continuum emission of L1527 IRS from OVRO. Contours are drawn at 3 mJy bm^{-1} intervals. Right: 2.7 mm continuum vector-averaged amplitudes of L1527 IRS. The dashed line shows the expectation value in absence of real signal; the solid line is a model fit of a point source plus an extended envelope.

C^{18}O 1–0, as well as $\lambda=3.4$ and 2.7 mm continuum emission were obtained at OVRO³, with typical synthesized beams of $5''$ (700 AU).

3. Occurrence of circumstellar disks

Interferometric observations are well suited to investigate the occurrence and growth of disks in the embedded class I phase (cf. Keene & Masson 1990; Terebey *et al.* 1993). Fig. 1 presents the OVRO 2.7 mm continuum measurements of the source L1527 IRS; the left panel shows the cleaned image, the right panel the vector-averaged visibility amplitudes. These amplitudes correspond to the Fourier components of the circular-symmetric part of the sky brightness distribution with respect to the source position, and are especially useful to separate extended and unresolved (i.e., $< 3'' \approx 420 \text{ AU}$) emission. The flux of the former decreases with increasing baseline separation, while that of the latter stays constant. Both components are clearly present in the measurements of L1527 IRS.

Six of our nine sources show point-source emission, presumably from circumstellar disks, with 2.7 mm fluxes ranging between 11 and 100 mJy. The flux levels toward the three remaining sources were insufficient to constrain the spatial distribution ($< 7 \text{ mJy bm}^{-1}$). The fact that $\geq 67\%$ of embedded YSOs show point-source emission implies that disks are formed very early in the star forming process, $\leq 10^4$ yr after the onset of collapse. No evidence for disk growth during the embedded phase of $\sim 10^5$ yr is found from our data, when comparing the results to the average 2.7 mm

³The Owens Valley Millimeter Array is operated by the California Institute of Technology under funding from the U.S. National Science Foundation (#AST93-14079).

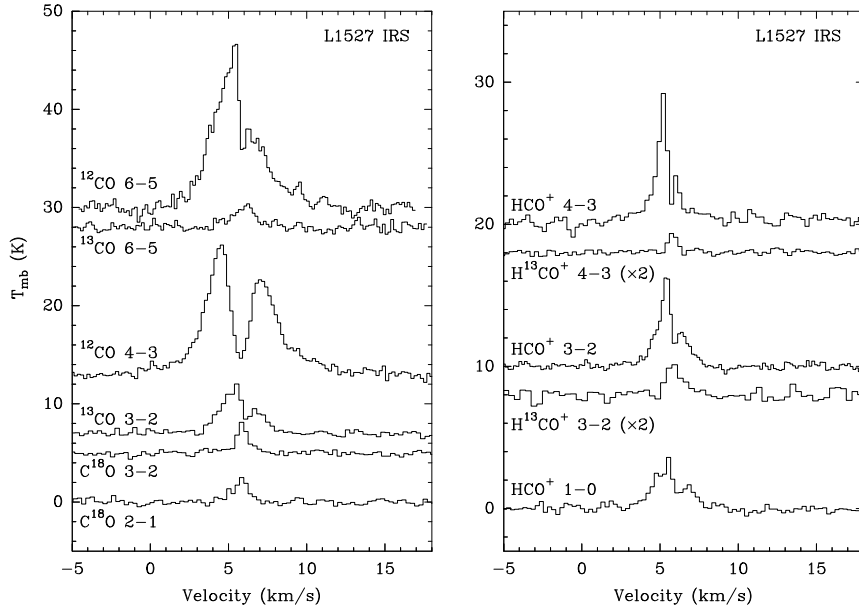


Figure 2. Single-dish ^{12}CO , ^{13}CO , C^{18}O , HCO^+ and H^{13}CO^+ spectra of L1527 IRS.

flux of ~ 24 mJy observed toward more evolved T Tauri stars with ages $\geq 10^6$ yr (Dutrey *et al.* 1996).

The disks are found to contribute 30–75% of the 1.1 mm single-dish flux measured by Moriarty-Schieven *et al.* (1994) in the $19''$ JCMT beam. The disk fluxes have been extrapolated using a spectral index of $\alpha = 2.5$, consistent with measurements of L1551 IRS 5, HL Tau and T Tau (Lay *et al.* 1994; Mundy *et al.* 1996; van Langevelde *et al.* 1997). Assuming an average dust temperature of 30 K and optically thin conditions, disk and envelope masses of 0.004 – $0.073 M_{\odot}$ and 0.004 – $0.26 M_{\odot}$, respectively, are inferred. Since the millimeter emission from the disks is likely to be moderately optically thick, it is concluded that the disks and the envelopes are typically equally massive in this phase, with each carrying $\sim 10\%$ of the mass of the central star (cf. Table 1).

4. Molecular observations of envelopes and outflows

Single-dish molecular line spectra of L1527 IRS are shown in Fig. 2. The line profiles are characterized by a line core of $\Delta V \approx 3 \text{ km s}^{-1}$, line wings originating in the bipolar outflow extending up to 10 km s^{-1} toward the red and the blue, and a $\sim 1 \text{ km s}^{-1}$ wide self-absorption feature due to cool material in the outer regions of the envelope. In the rarer isotopic species like H^{13}CO^+ and C^{18}O only the line core is sampled. Such spectra

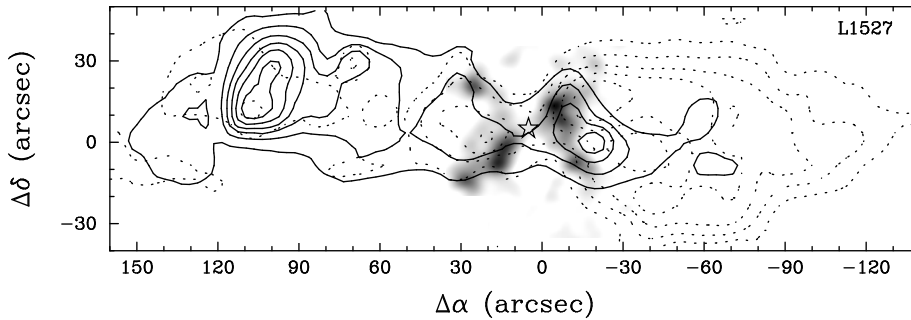


Figure 3. Integrated HCO^+ 1-0 intensity observed toward L1527 IRS with OVRO (grey scale) superposed on the red (dashed contours) and blue (solid contours) ^{12}CO 3-2 outflow lobes (from MacLeod *et al.* 1994).

can be used to test models of protostellar collapse (e.g., Terebey, Shu & Cassen 1984; Galli & Shu 1993; Foster & Chevalier 1993) through a careful treatment of the radiative transfer and the molecular excitation (cf. Zhou *et al.* 1993; Walker, Narayanan & Boss 1994; Choi *et al.* 1995).

Comparison between the millimeter continuum fluxes and the integrated HCO^+ and H^{13}CO^+ line intensities shows that HCO^+ 3-2 and 4-3 are particularly good tracers of the envelopes of our sources. The envelope density distribution is found to follow a radial power law with a slope between 1 and 3, consistent with collapse models.

In the OVRO beam, the HCO^+ , ^{13}CO , and C^{18}O emission traces rotation in the equatorial regions of the envelopes, as well as material closely connected with the cavities cleared by the outflow. The best example of this is offered by L1527 IRS (Fig. 3), where the integrated HCO^+ emission outlines the red and blue outflow lobes. Whether the outflow actively compresses the material along the cavity walls, or merely provides a low-opacity pathway for heating radiation from the central object to reach into the envelope (cf. Spaans *et al.* 1995) remains subject of further investigation.

5. Conclusions

The emission of dust and molecules provides complementary views of the young stellar environment. A detailed study of nine embedded, low-mass YSOs shows that (1) circumstellar disks are formed early in the star formation process and occur around at least two-thirds of all YSOs, (2) HCO^+ 3-2 and 4-3 are excellent tracers of the envelopes, and (3) the bipolar outflow has a profound influence in shaping the appearance of the envelopes on 1000 AU scales.

MRH gratefully acknowledges financial support from the *Stimuleringsfonds Internationalisering* of the Netherlands Organization for Scientific Research (NWO) and from the organizers of this School.

References

1. André, Ph., & Montmerle, T. (1994) From T Tauri stars to protostars: Circumstellar material and young stellar objects in the ρ Ophiuchi cloud. *ApJ*, **420**, pp. 837–862
2. Beckwith, S. V. W., Sargent, A. I., Chini, R. S., & Güsten, R. (1990) A survey for circumstellar disks around young stellar objects. *AJ*, **99**, pp. 924–945
3. Chandler, C. J., Sargent, A. I. (1997) The role of dust in star and planet formation: observations. in *From dust to Planetesimals*, eds. Y. J. Pendleton, A. G. G. M. Tielens, (San Francisco: ASP), in press.
4. Choi, M. H., Evans II, N. J., Gregersen, E. M., & Wang, Y. S. (1995) Modeling line profiles of protostellar collapse in B335. *ApJ*, **448**, pp. 742–747
5. Dutrey, A., Guilloteau, S., Duvert, G., Prato, L., Simon, M., Schuster, K., Menard, F. (1996) Dust and gas distribution around T Tauri stars in Taurus–Auriga. I: Interferometric 2.7 mm continuum and ^{13}CO $J=1-0$ observations. *A&A*, **309**, pp. 493–504
6. Foster, P. N., & Chevalier, R. A. (1993) Gravitational collapse of an isothermal sphere. *ApJ*, **416**, pp. 303–311
7. Galli, D., & Shu, F. H. (1993) Collapse of magnetized molecular cloud cores. I: Semi-analytical solution. *ApJ*, **417**, pp. 220–242
8. Hogerheijde, M. R., van Dishoeck, E. F., Blake, G. A., & van Langevelde, H. J. (1997) Tracing the envelopes around embedded low-mass young stellar objects with HCO^+ and millimeter-continuum observations. *ApJ*, in press.
9. Keene, J., & Masson, C. R. (1990) Detection of a 45 AU radius source around L1551 IRS 5: A possible accretion disk. *ApJ*, **355**, pp. 635–644
10. Lada, C. J. (1987) Star formation: from OB associations to protostars. in *Star Forming Regions*, eds. M. Peimbert, J. Jugaku (Dordrecht: Reidel), pp. 1–17
11. Lay, O. P., Carlstrom, J. E., Hills, R. E., & Phillips, T. G. (1994) Protostellar accretion disks resolved with the JCMT–CSO interferometer. *ApJ*, **434**, pp. L75–L78
12. MacLeod, J., Lorne, A., Harris, A., Tacconi, L., & Schuster, K. (1994) Extended CO 6–5 emission from a nearby outflow source. *JCMT Newsletter*, Sept./Oct. 1994
13. Moriarty-Schieven, G. H., Wannier, P. G., Keene, J., & Tamura, M. (1994) Circum-protostellar environments II. *ApJ*, **436**, pp. 800–806
14. Mundy, L. G., Looney, L. W., Erickson, W., Grossman, A., Welch, W. J., Forster, J. R., Wright, M. C. H., Plambeck, R. L., Lugten, J., & Thornton, D. D. (1996) Imaging the HL Tauri Disk at $\lambda = 2.7$ mm with the BIMA array. *ApJ*, **464**, pp. L169–L173
15. Osterloh, M., & Beckwith, S. V. W. (1995) Millimeter-wave continuum measurements of young stars. *ApJ*, **439**, pp. 288–302
16. Spaans, M., Hogerheijde, M. R., Mundy, L. G., van Dishoeck, E. F. (1995) Photon heating of YSO envelopes as an explanation for CO 6–5. *ApJ*, **455**, pp. L167–L170
17. Tamura, M., Gatley, I., Waller, W., & Werner, M. W. (1991) Two micron morphology of candidate protostars. *ApJ*, **374**, pp. L25–L28
18. Terebey, S., Shu, F. H., & Cassen, P. (1984) The collapse of the cores of slowly rotating isothermal clouds. *ApJ*, **286**, pp. 529–551
19. Terebey, S., Chandler, C. J., & André, Ph. (1993) The contribution of disks and envelopes to the millimeter continuum emission from very young low-mass stars. *ApJ*, **414**, pp. 759–772
20. van Langevelde, H. J., van Dishoeck, E. F., & Blake, G. A. (1997) Dust and CO in the T Tauri circumstellar matter. in *CO: Twenty-five Years of Millimeter-wave Spectroscopy*, eds. W. B. Latter et al. (Dordrecht: Kluwer), p. 469
21. Walker, C. K., Narayanan, G., & Boss, A. P. (1994) Spectroscopic signatures of infall in young protostellar systems. *ApJ*, **431**, pp. 767–782
22. Zhou, S., Evans II, N. J., Kömpe, C., & Walmsley, C. M. (1993) Evidence for protostellar collapse in B335. *ApJ*, **404**, pp. 232–246